International Journal of Engineering Research & Technology (IJERT)
ISSN: 2278-0181
Vol. 15 Issue 09 , September - 2026

Investigating The Effect of Geomagnetic Cutoff Rigidity on Forbush Decrease

Otukaoha Collins Uche, Chima Abraham Iheanyichukwu and Anochili Lydia Uchenna
Department of Industrial Physics, Enugu State University of Science and Technology, Agbani

Abstract - Investigation on the effect of geomagnetic cutoff rigidity on Forbush decrease has been successfully conducted. This was done using cosmic rays daily counts from Tibet (TIBT) and Magadan (MGDN) Cosmic Ray (CR) station. Data of Interplanetary Magnetic Field (IMF) was equally used for the study. These data span a period of four years from the year 2013 to 2015. The data were analyzed using R. statistical software. The results of our analysis was grouped into station of high and low cutoff rigidity. A sharp depression in the intensity of cosmic ray intensity variations known as Forbush Decrease (FD) was detected. Advanced manual approach was used to select the FDs. A large number of FDs were recorded. The MGDN CR station which represents station of low rigidity recorded the highest number of FDs with a total of 898 events followed by TIBT CR station representing station of high cutoff rigidity with a total of 388 events. The magnitude of these FDs was determined. They were further listed and presented as FD catalogue. It was observed that FD magnitudes vary inversely with the stations rigidity. A correlation between the magnitudes of the two stations was also carried out. A strong and positive correlation with a value cc = 0.79 was observed between the FD magnitudes of the two stations. Lastely, a correlation between FD magnitudes and interplanetary magnetic field was tested. The result of the correlation indicated a weak and positive value of cc = 0.27 and cc = 0.29 for TIBT and MGDN FD magnitudes respectively. This signifies that IMF is among the influence the magnitude of the FDs.

KEYWORDS:Cosmic rays,Forbush decrease,geomagnetic cutoff

1.INTRODUCTION

The groundbreaking observation of Cosmic Ray (CR) variations has highlighted the phenomena associated with abrupt changes in CR flux intensity. These short-term intensity variations, typically linked to disturbances from solar wind, are commonly known as Forbush Decreases (FD) (Lee *et al.,* 2015). During an FD, there is a rapid decrease in CR intensity (Lee *et al.,* 2015). This swift decrease is primarily caused by strong magnetic boundaries that act against CR particles, which are generated by Interplanetary Coronal Mass Ejections (ICMEs) (Cane, 2000) and Interplanetary Shocks (IP shocks) that occur near Earth (Lockwood *et al.,* 1991a). Additionally, FDs may arise when magnetic clouds interact closely with the Earth (Lee *et al.,* 2008). Further contributing factors to FDs include magnetic-field variations associated with the interplanetary shock-sheath region (Lockwood *et al.,* 1991b) and specific magnetic clouds (Badruddin, 2002). Notably, FDs generally follow well-defined profiles that consist of four distinct stages: onset, main phase, maximum depression point, and recovery phase. This structured progression begins with a main phase marked by decreasing CR intensity and transitions into a recovery phase where CR intensity begins to rebound, thereby creating a recognizable FD time profile (Lee *et al.,* 2013). The complete FD profile can span anywhere from a few hours to several days, illustrating the dynamic nature of these cosmic events (Lee *et al.,* 2008).

During FDs, the trajectories of cosmic ray particles are curved by the Earth’s magnetic field (Bütikofer, 2018). The ability of these CR particles to penetrate magnetic fields and reach the upper atmosphere of the Earth is governed by Rigidity (R), which is defined as the particle’s momentum multiplied by the speed of light divided by its charge (Kalugin and Kabin, 2015). The concept of geomagnetic cutoff rigidity serves to illustrate how Earth's magnetic field protects against the influx of charged cosmic ray particles from outside the magnetosphere (Shea and Smart, 2006). This cutoff rigidity is typically expressed in gigavolts (GV) (Kalugin and Kabin, 2015). It is a common misconception that rigidity values are fixed (Shea and Smart, 2006). In reality, these values can fluctuate due to changes in both dipole and non-dipole components of the magnetic field (Shea and Smart, 2006). Consequently, alterations in geomagnetic cutoff rigidity directly impact the magnitude of CRs that strike the atmosphere at any given location over time (Shea and Smart, 2006). Understanding these dynamic changes is crucial for grasping how cosmic rays interact with Earth’s environment.

Research highlights the significant role of geomagnetic cutoff rigidity and geographic coordinates in influencing Forbush Decreases (FDs). For instance, Webber (1962) provided valuable insights by demonstrating that following three notable decreases in July 1959, the total integral intensity of CR particles with rigidities above approximately 1 GV at Earth reduced to just 20% of the intensity observed during sunspot minimum, a period when CR intensity typically peaks. Building on this foundation, Lockwood and Webber (1991b) advanced our understanding by employing two distinct methodologies to explore the rigidity dependence of

International Journal of Engineering Research & Technology (IJERT)
ISSN: 2278-0181
Vol. 15 Issue 09 , September - 2026

FDs through changes in neutron monitor counting rates. Their approaches included analyzing the IMP>60MeV rate and utilizing different energy channel rates from IMP, thus enriching our grasp of FDs' behavior.
Pyle (1997) further contributed to this field by examining a single FD, revealing that the degree of solar modulation's effect on galactic flux at Earth, above ~1 GV, is inversely related to the rigidity of the particles. This relationship underscores the complexity of interactions within space weather phenomena. Additionally, Jamsen *et al.* (2007) investigated energy dependence in the recovery time of FDs across three events, emphasizing the strong correlation between recovery time and energy levels. Similarly, Lingri *et al.* (2016) reinforced these findings by analyzing three events and demonstrated that each neutron monitor records FDs in accordance with the specific cutoff rigidity of its location. Collectively, these studies offer a comprehensive understanding of the interactions between cosmic rays and solar activity, laying the groundwork for further exploration in this crucial area of space science.
In view of this study, we shall use a large number of FDs from two neutron monitor stations (NMs) to test the rigidity dependence of FDs.

2.MATERIALS

The major materials that was used for this study are the daily CR data that was obtained from http://cr0.izmiran.ru/common/ for the CR stations including TIBT and MGDN. This data covered the period of three years between the years 2013 to 2015. The data on IMF was also used and sourced from https://omniweb.gsfc.nasa.gov/html/owdata.html for the same period of three years (2013-2015). R. statistical software is used for the statistical analysis.

2.1.Methods

The methods applied in this research are grouped under the following subsections;

2.1.2.Data Source

The daily data for cosmic rays was systematically harvested from the IZMIRAN website across the two cosmic ray stations for the designated study period. To facilitate analysis, this data was organized using text editor software. During this process, records for 00 were excluded, allowing us to focus solely on daily counts. The resulting dataset now features a clear tabular format that includes only the relevant dates and cosmic ray counts, with each neutron station's data saved under a unique file name for easy reference.
Similarly, interplanetary magnetic field data was also obtained from online resources and structured in the same tabular format. This additional data covers the same time frame as that of the cosmic rays. Careful filtering ensured that only pertinent dates and counts were included during the download phase, utilizing the website's data query features. Each dataset was saved with distinct file names to maintain organization and accessibility.

2.2.Processing of Data

In this study, the advanced manual method was employed for FD selection, utilizing a computer program integrated with R statistical software. The following outlines the processes and stages involved in this method, highlighting its structured approach:
(a) The program reorganizes raw CR data into a distinct format that includes unique dates and corresponding counts. It then saves this information with a uniquely designated filename.
(b) The program reads the file saved in (a) and scale it to plot daily variations in the CR counts for the study period.
(c) The program normalizes the daily CR counts using

$$V = \frac{y - mean\,(y)}{mean\,(y)} * 100 \quad (1)$$

where y = CR counts.
(d) The program then generates a plot of the normalized CR counts against dates, demonstrating decreases in the variations of CR counts. This provides a baseline for FD detection, illustrated by an ab-line that highlights the changes in CR variations.
(e) A threshold of less than -0.5% was established as the baseline for selecting FD magnitude.
(f) The program proceeds to filter the observed variations for the first time, marking them with red points for clarity.
(g) For a second round of filtering, the program incorporates the identified FD dates and magnitudes, enabling a clearer representation of FDs in the subsequent plot.
The dates and magnitudes of FDs was compiled and presented in a structured format. The FD dates was listed separately in a table, followed by a comprehensive FD catalog detailing their respective magnitudes. These FDs was categorized into three phases based on the cut-off rigidity of their respective neutron stations: high, low, and middle rigidity. Each category was displayed in tabular form. Additionally, the IMF data will be aligned alongside the FD information, also presented in tables for clarity. The complete dataset was fully documented in the appendix.
A correlation test was conducted between selected FD magnitudes and the stations' geomagnetic cut-off rigidity, with the results illustrated in a correlation plot. Both the geomagnetic cut-off rigidity values and FD magnitudes was summarized in tabular format. Further analysis will involve testing the correlations between FD magnitudes across different stations, categorized by their high, low, and middle cut-off rigidity. A table containing the correlation coefficients was included, along with the corresponding plots. Lastly, a correlation analysis was performed between FD magnitudes and IMF, with the results documented in a correlation table and accompanying plots.

International Journal of Engineering Research & Technology (IJERT)
ISSN: 2278-0181
Vol. 15 Issue 09 , September - 2026

3.0.RESULTS

3.1.Selection of FDs

The variation of Fig 1.1 shows the raw daily cosmic ray count while Figs 1.2 and 1.3 show the filtration of the cosmic ray data to indicate better points of FDs. The selected FDs from two CR stations of TIBT and MGDN were grouped into two categories as stations of high and low cut-off rigidity. The samples of the selected FD dates are shown in Tables 1.1 and 1.2 while the complete results are shown in Appendix.

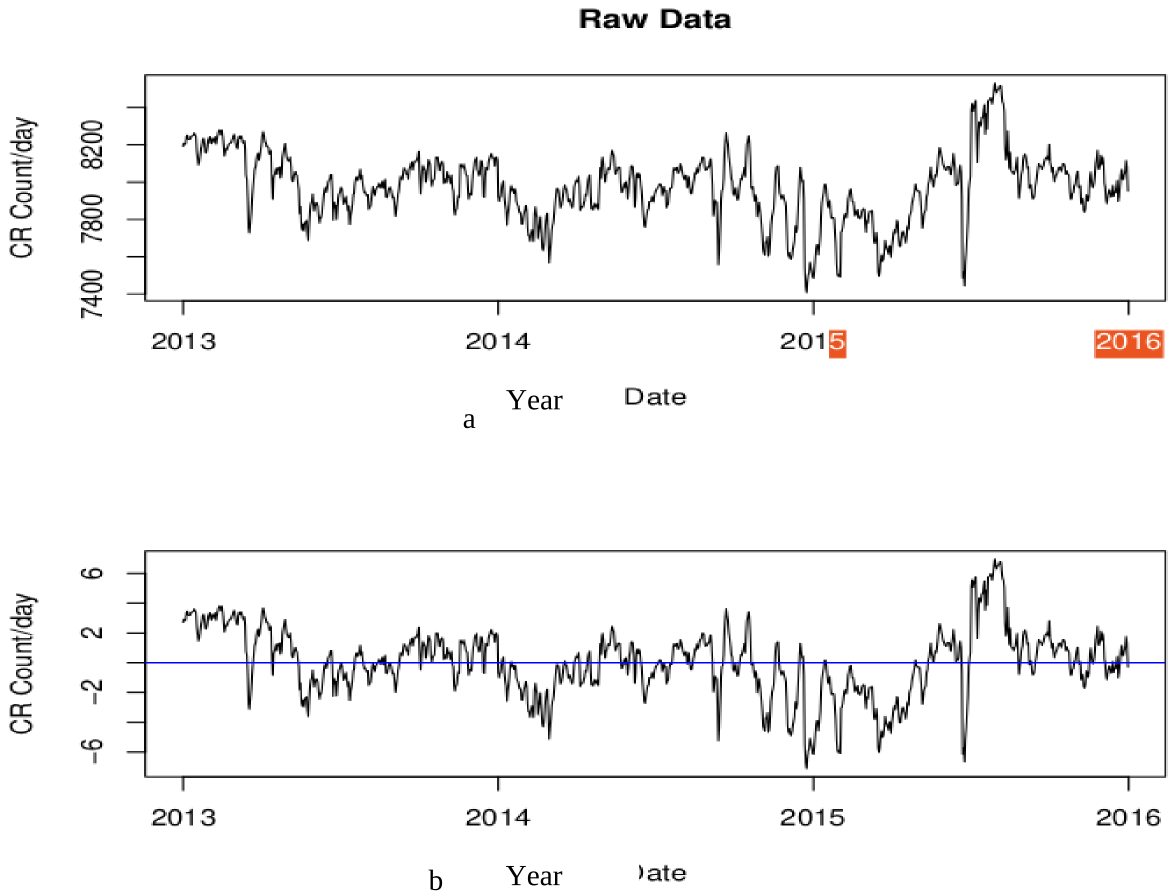

Fig 1.1: (a) Variations of cosmic ray raw data. (b) Variations of cosmic ray raw data showing a baseline for FD selection

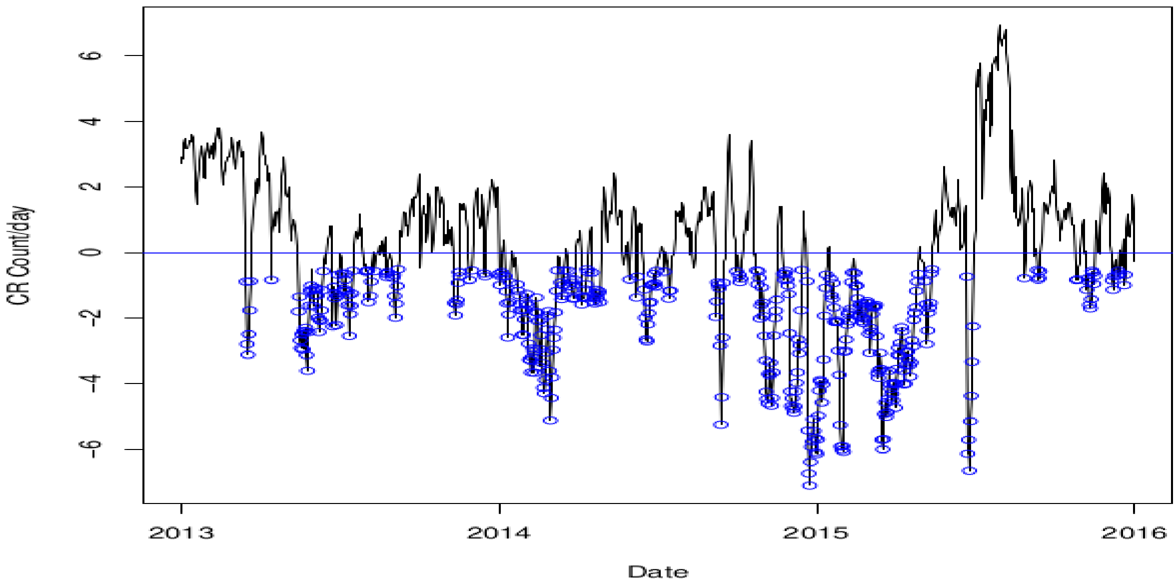

Year

Fig. 1.2: First filtration of CR data

International Journal of Engineering Research & Technology (IJERT)
ISSN: 2278-0181
Vol. 15 Issue 09 , September - 2026

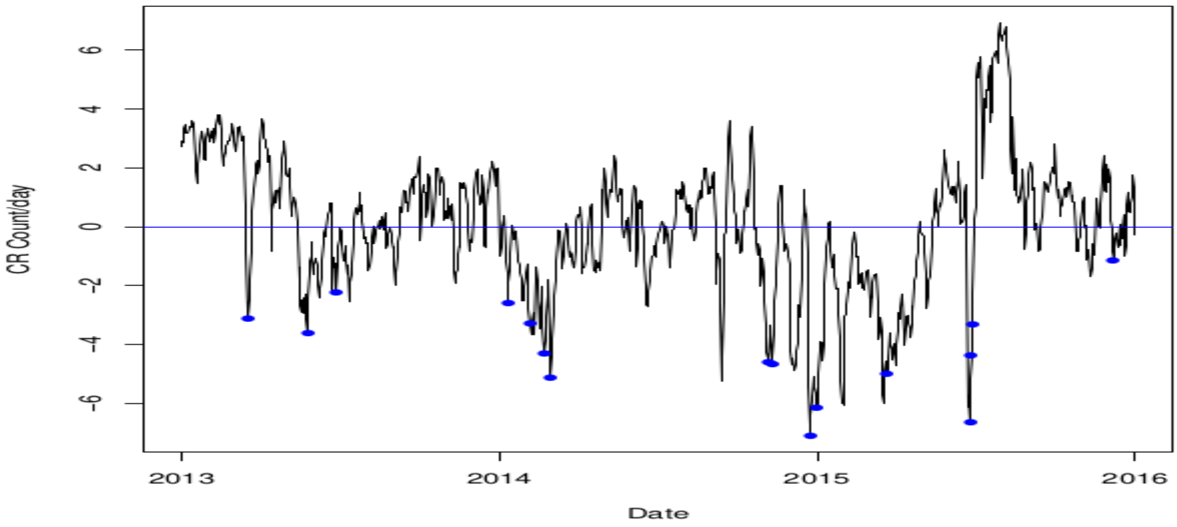

Year

Fig. 1.3: Second filtration of CR data

Selected FDs for CR station of High Cutoff Rigidity

Sample of the selected FD dates for station of high cutoff rigidity are shown in Table 1 below while the complete data are shown in Appendix I. The TIBT CR station represents the station of high cutoff rigidity. The first column in Table 1 contains the serial number followed by the event date of TIBT CR station. A total of 388 FDs were observed in the TIBT CR station.

Table 1.1: Selected FD Dates for TIBT CR Station

S/N	DATE
(a)	(b)
1	2013-03-16
2	2013-03-17
3	2013-03-18
4	2013-03-19
5	2013-03-20
6	2013-03-21
7	2013-03-22
8	2013-03-23
9	2013-04-14
10	2013-04-15
11	2013-04-16
12	2013-04-17
13	2013-04-18
14	2013-04-19
15	2013-05-15
16	2013-05-16
17	2013-05-17
18	2013-05-18
19	2013-05-19
20	2013-05-20
21	2013-05-21

International Journal of Engineering Research & Technology (IJERT)
ISSN: 2278-0181
Vol. 15 Issue 09 , September - 2026

22	2013-05-22
23	2013-05-23
24	2013-05-24
25	2013-05-25
26	2013-05-26

1.1.Selected FDs for CR station of low cutoff rigidity

Sample of the selected FD dates for station of low cutoff rigidity are shown in Table 1.2 below . The MGDN CR station represents the station of high cutoff rigidity. The first column in Table 2 contains the serial number followed by the event date of MGDN CR station. A total of 898 FDs were observed in the MGDN CR station.

Table 1.2: Selected FD Dates for MGDN CR Station

S/N	DATE
1	2013-01-19
2	2013-01-20
3	2013-03-15
4	2013-03-16
5	2013-03-17
6	2013-03-18
7	2013-03-19
8	2013-03-20
9	2013-03-21
10	2013-03-22
11	2013-03-23
12	2013-03-24
13	2013-03-25
14	2013-03-26
15	2013-03-27
16	2013-03-30
17	2013-04-14
18	2013-04-15
19	2013-04-16
20	2013-04-17
21	2013-04-18
22	2013-04-19
23	2013-04-20
24	2013-04-21
25	2013-04-22
26	2013-04-23
27	2013-04-24

Determined FD Magnitudes

Tables 1.3 and 1.4 and Appendix II show the determined FD magnitude for stations of high and low cutoff rigidity respectively.

Determined FD magnitudes for high cut-off rigidity stations

Samples of determined FD magnitudes for TIBT CR station which represents the stations of high rigidity are shown in Table 1.3 below .

Table 1.3: Determined FD magnitudes for TIBT CR Station

S/N	TIBT DATE	FD MAG (%)	IMF

Published by :
https://www.ijert.org/
An International Peer-Reviewed Journal

International Journal of Engineering Research & Technology (IJERT)
ISSN: 2278-0181
Vol. 15 Issue 09 , September - 2026

1	2013-03-16	-0.59	5.5
2	2013-03-17	-0.81	10
3	2013-03-18	-1.66	9.5
4	2013-03-19	-1.87	6.8
5	2013-03-20	-1.39	6.4
6	2013-03-21	-0.81	6.6
7	2013-03-22	-0.81	5.1
8	2013-03-23	-0.52	5
9	2013-04-14	-0.96	10.8
10	2013-04-15	-1.34	8.8
11	2013-04-16	-0.91	4.5
12	2013-04-17	-0.86	3.4
13	2013-04-18	-0.8	3.4
14	2013-04-19	-0.61	4
15	2013-05-15	-0.71	7.7
16	2013-05-16	-1.5	5.9
17	2013-05-17	-1.46	5.8
18	2013-05-18	-1.71	8.6
19	2013-05-19	-1.44	5.5

Determined FD magnitudes for low cutoff rigidity stations

Sample of determined FD magnitudes for MGDN CR station which represents the stations of low cutoff rigidity are shown Tables 1.4 below and Appendix IV. Their corresponding IMF data are equally shown in the table.

Table 1.4: Determined FD magnitudes for MGDN CR Station

	MGDN		
S/N	DATE	FD MAG (%)	IMF
1	2013-01-19	-0.9	4.8
2	2013-01-20	-0.74	4.9
3	2013-03-15	-1.59	8.4
4	2013-03-16	-1.86	5.5
5	2013-03-17	-3.2	10
6	2013-03-18	-5.06	9.5
7	2013-03-19	-5.38	6.8
8	2013-03-20	-4.76	6.4
9	2013-03-21	-4.05	6.6
10	2013-03-22	-3.19	5.1
11	2013-03-23	-2.46	5
12	2013-03-24	-1.79	3
13	2013-03-25	-1.16	4.4
14	2013-03-26	-1.08	3.7
15	2013-03-27	-0.6	7.7
16	2013-03-30	-0.59	4.3
17	2013-04-14	-1.95	10.8
18	2013-04-15	-3.15	8.8
19	2013-04-16	-1.76	4.5
20	2013-04-17	-1.53	3.4
21	2013-04-18	-1.37	3.4

International Journal of Engineering Research & Technology (IJERT)
ISSN: 2278-0181
Vol. 15 Issue 09 , September - 2026

22	2013-04-19	-1.14	4
23	2013-04-20	-1.53	4.1
24	2013-04-21	-1.12	5
25	2013-04-22	-1.2	4.6
26	2013-04-23	-1.04	7.5
27	2013-04-24	-1.75	12.6
28	2013-04-25	-1.5	6.1

Correlation Test

The correlations were gotten using a general Pearson correlation formula;

$$r = \frac{\sum_{j=1}^{k}(x_j-\bar{x})(y_j-\bar{y})}{\sqrt{\sum_{j=1}^{k}(x_j-\bar{x})^2(y_j-\bar{y})^2}} \quad (2)$$

(Okwonu *et al.*, 2020)

where r = correlation coefficient, $\bar{x} = \frac{\sum_{j=1}^{k} x_j}{k}$, and $\bar{y} = \frac{\sum_{j=1}^{k} y_j}{k}$ are the sample means. Note that $(x_j, y_j, j = 1, \ldots \ldots, n)$ are data points from two variables assumed to be normally distributed with parameters $\mu^x, \mu^y, \delta_\mu^2 x, \delta_\mu^2 y$.

The correlations are grouped into two phases. Phase one shows the correlation between the FD magnitudes of the two CR stations while phase two shows the correlation between the FD magnitudes and their corresponding interplanetary magnetic field data. Pearson r correlation method was used for the correlation test. The results of these correlations are shown with tables and plots.

Correlations between FDs of the two CR stations

The result of the correlation between FD magnitudes of two CR stations is shown in Fig. 1.5 below.

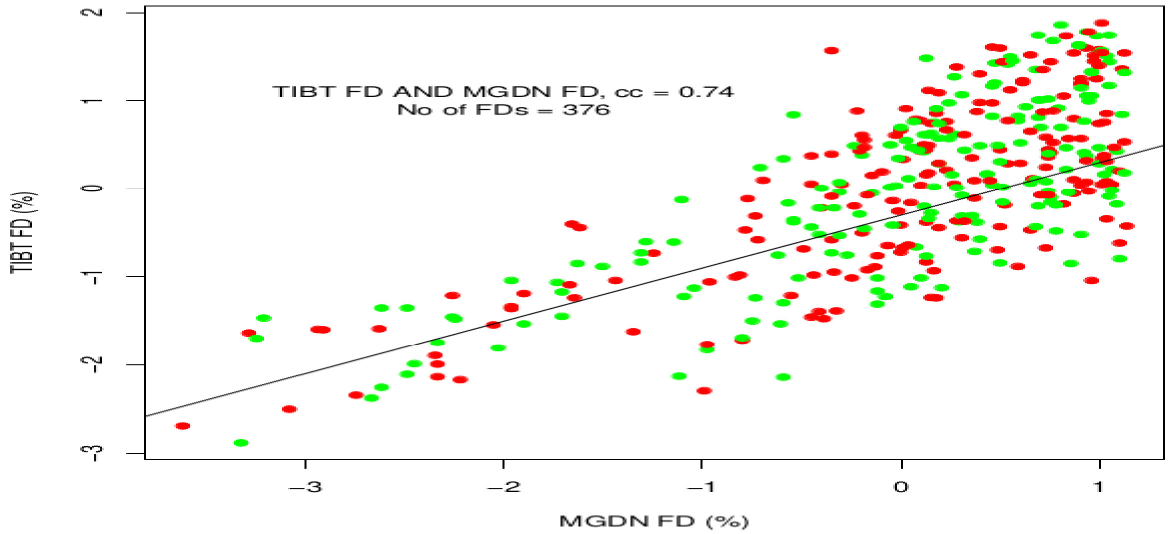

Fig 1.4: Correlation plot of the FD magnitudes of TIBT and MGDN CR stations

Correlation between FDs and IMF

The correlation of FD magnitudes and their corresponding interplanetary magnetic field data are grouped into two. The first group stands for station of high rigidity while the second stands for station of low cutoff rigidity respectively. Pearson r correlation method was used for the correlation test. Fig. 6 and 7 shows the correlation plots of TIBT and MGDN CR stations which represents stations of high and low cutoff rigidity respectively.

International Journal of Engineering Research & Technology (IJERT)
ISSN: 2278-0181
Vol. 15 Issue 09 , September - 2026

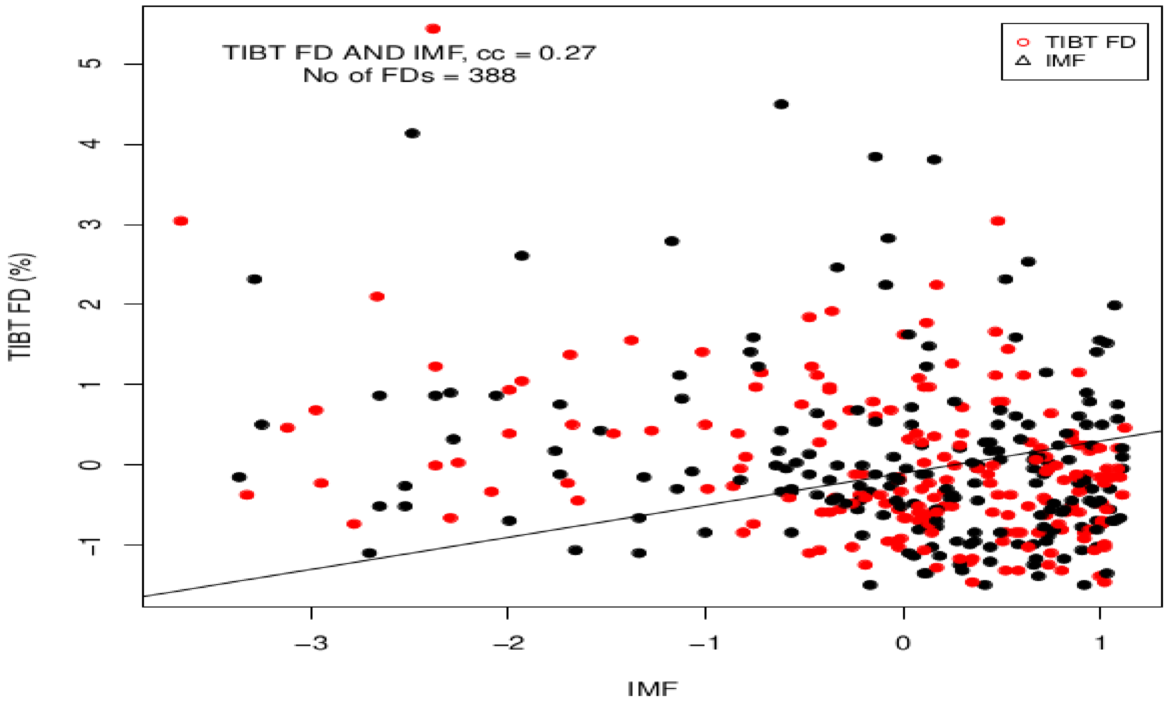

Fig. 1.5. Correlation plot of TIBT FD with IMF

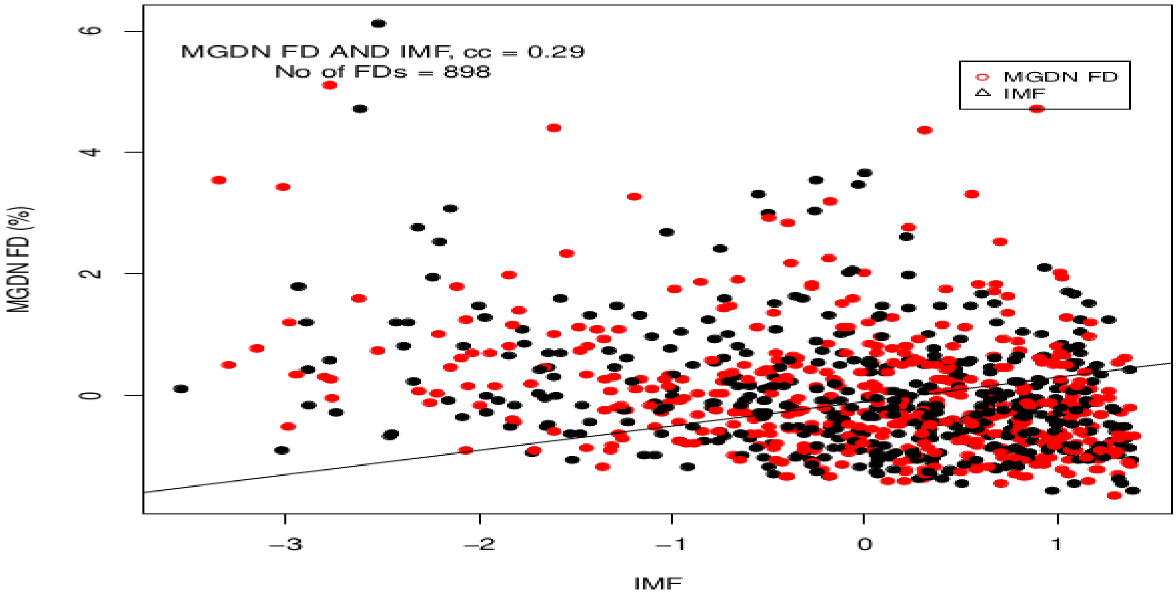

Fig. 1.6: Correlation plot of MGDN FD with IMF

4.0.DISCUSSION

4.1Selection of FDs

The manual method of FD selection involves a number of stages: (a) Defining a certain threshold or baseline. (b) reduction in CR flux intensity. (c) Normalizing CR intensity data using a chosen running mean. (d) Trial and error method, involving plotting CR data for some equal intervals of time, calculating the percentage change (with reference to the running mean) of the normalized CR data at the onset time and the percentage change at the time of maximal depression, min (e) Subtracting I from I and deciding whether I - min max min I ≥B, max (f) Deciding the events for which I - I ≥ B (that min max will qualify for FDs) and the rest discarded as non-FD event and, (g) Estimating either the onset time or time of maximal decreases of all the events that meet the condition in (see Harrison & Ambaum, 2010; Kristjansson *et al.*, 2008; Oh, Yi, and Kim, 2008, for details of the approach). A close inspection of Figure 1 by Harrison and Ambaum (2010) suggests that each of the steps is subject to several potential biases.

The automated method differs significantly from the manual technique. The automated method uses a program that views CR data as a Fourier series and thus, transforms CR data using the Fourier Transform Technique (FTT). While the manual approach involves

International Journal of Engineering Research & Technology (IJERT)
ISSN: 2278-0181
Vol. 15 Issue 09 , September - 2026

the tedious and time-consuming task of culling and plotting CR data for a few selected days, judging whether the plotted data reflect a typical FD profile, examining the various parts of the plotted FD such as onset time, main phase, and time of maximal depression, calculating the level of intensity increases or reductions and so on, the automated method handles the CR data as a single signal, irrespective of the volume. After the Fourier transformation and filtering of the unwanted signals, a script for FD event identification is written in an R language for statistical computing (R. Core Team, 2014). The algorithm takes the Fourier-transformed signal as its input data. It scans the data, picking all the pits/peaks/depressions/troughs. Another subroutine identifies the time of the depressions/peaks and passes the results to some subprograms that perform several other tasks such as determining the static mean of the input data, isolating pits from peaks, estimating the amplitude of the depressions with reference to the calculated average, and so on.
However, the FDs obtained from these methods are subject to validation. For instance, Kristjansson *et al.* (2008), identified 22 large FDs between 2000 and 2005 using Climax data. They validated the dates of these events by comparing them with FDs found in another two stations, the Oulu and Moscow stations. An event is said to be an FD if the CR data are equal to or lower than a certain baseline for instance 5% below the 90-day running mean.

Tables 1.1 and 1.2 show a sample of the selected FDs in this work while the complete data is shown in Appendix I. The selected FDs were grouped into two which include stations of high and low rigidity. The FDs of the station of high rigidity were presented in Table 1, while those of low are presented in Tables 1.2. From Table 1.1, it was observed that the TIBT station recorded 388 FDs. The TIBT CR station was used to represent the station of high rigidity. From Table 1.2 and Appendix II in extension, a total of 898 FDs were recorded for MGDN CR station. The MGDN CR station was used to represent the stations of low rigidity. A close study and comparison of the event date selection of the two tables indicated some variations. While the station with low cut-off rigidity consistently recorded the highest number of FDs, the station with high cut-off rigidity recorded the least number of FDs. For instance, while the MGDN station which is of low rigidity recorded 898 FDs, TIBT which is of high cut-off rigidity was recording 388 FDs. This finding is in agreement with Belov *et al.* (2021), which suggested that the amplitude of the FDs was found to decrease as the rigidity increased.

However, because altitude and rigidity determine the sensitivity of NMs, the trade-off between the stronger rigidity of TIBT and the smaller rigidity of MGDN is expected to result in similar detection efficiency. This is in agreement with the result obtained. Some event dates were observed to be similar. These similar dates are summarized in Appendix II. These similar dates validate our result since research had proven that stations of similar rigidity mostly produce simultaneous FDs.

These FD tables were used to form FD catalogues. A catalogue of FDs is a list of computed FDs containing the FD magnitudes and their corresponding magnitudes. This FD catalogue forms a database for FD researchers. The data presented in the catalogue may be useful to a number of researchers, including those analyzing the relation between FDs and their solar sources, the impact of CRs on terrestrial weather, or the global simultaneity of FDs. The data were presented in such a manner that almost every CR investigator can employ it directly in analysis. The event magnitude and date are presented and can be used for either superposition or correlation analysis.

4.2 Determination of FD Magnitudes
The magnitude of an FD is the strength of the depression in cosmic ray intensity variation. Tables 1.3 and 1.4 show the determined FD magnitudes for CR stations of high and low cutoff rigidity respectively. Previous research has shown that the magnitude of FDs depends on the rigidity of neutron monitors. For instance, Belov *et al.* (2021), suggested that as a general trend, the amplitude of the FDs was found to decrease as the rigidity increased. Tables 1.3 and 1.4 of this study show the FD magnitudes according to high and low rigidity. It was observed that the MGDN station of low rigidity recorded a highest magnitude of FDs. For instance, the highest FD was recorded on 29-12-2014 with a magnitude of -9.27% for the MGDN station which has a low rigidity of 2.11 GV. Generally, the stations with low rigidity produce a greater number of FD magnitudes. However, the small FDs do not show a very deep depression. These small FDs are sometimes seen to be the non-simultaneous (Oh *et al.*, 2008; Okike and Collier, 2011a)
i.e FD types that are not usually observed by all the stations. Tezari and Mavromichalaki (2016) suggested that these small events are affected by diurnal anisotropy, unlike the large ones. On contrary, the stations with high rigidity had low FD magnitudes. For instance, the lowest FDs were detected on 28-01-2014 and 06-10-2015 which had a magnitude of -0.50% and -0.51% respectively for TIBT which has a high rigidity of 14.10 GV. However, the station with high rigidity produce a lesser number of FD magnitudes. For instance, the TIBT station recorded a total of TIBT station recorded 388 FDs. This also confirms the assertion of Belov *et al.*, (2021) that the amplitude of the FDs was found to decrease as the rigidity increased. Generally, large Forbush events tend to show a clear deep depression.

4.2.Correlation Test
A good correlation was found to exist between the FD magnitudes of the stations and rigidity. Fig. 1.5 shows the correlation plots of the FDs of these stations according to high and low rigidity. A correlation coefficient of cc = 0.76 was found for TIBT, and MGDN CR station. A total of 376 events which were simultaneous for the two stations were used for this plot. The correlation indicates that it is strong and positive since the plotted points are clustered around the line of best fit and the correlation value equally high. This finding is in agreement with the suggestion that the magnitude of FDs is rigidity dependent. Also, our results are in agreement with

the suggestion of Okike and Nwuzor (2020) that the FDs measured at the stations can be used to examine the effects of rigidity between the two stations. However, Todd and Kniveton (2001) analyzed FDs at three high-latitude stations (NWRK, MCMC, and SOPO). Although they did not indicate the outcome of their comparison nor the implication of the result obtained, the general underlying assumption among researchers conducting FD-based correlation/regression or epoch investigation is that FDs that are simultaneous at two or more stations are strong events. Between the years 2000 and 2005, Kristjansson *et al.* (2008) selected 22 FDs using CLMX data, and following the same approach, they simply stated that their FD event days were compared with those at Oulu and Moscow NMs, and by extension, they assumed that their FDs are consistent, or rather simultaneous.

Research has equally shown that a correlation exists between FD magnitude and solar parameters. Belov *et al*, (2001) reveal that the correlation between FD magnitude and the product of the magnetic field enhancement and the SW speed increase is better than correlations for the two SW parameters treated separately. Therefore, we analyzed correlations of FD magnitudes with the solar wind speed (SWS) and interplanetary magnetic field (IMF) data to find out which of these solar parameters is the most relevant to FDs. The results of the correlations are presented in Fig 1.6 and 1.7. Fig 1.6 shows the correlation between TIBT FDs and IMF while Fig 1.7 shows that of MGDN FDs and IMF. A weak and positive correlation was observed with correlation values cc = 0.29 and cc = 0.27 for TIBT with IMF and MGDN with IMF respectively. The alignment of the plotted points around the line of best fit is equally a good indication of weak correlation.

Generally, it was observed that IMF has a stronger correlation with the FD magnitudes of these stations. This signifies that IMF is among the causative agents of FDs.

5.0.SUMMARY

5.1.Summary of Findings

The summary of this research is presented in line with the objectives and corresponding results and discussion which are stated as follows.

The advanced manual method of FD selection used in this research identified new FDs. A large number of FDs were identified by this research. These identified FDs were used to form a catalogue of FDs to contribute our quota to FD research.

An R.-based program was used to determine the selection and magnitude of FDs. Stations with lesser rigidity were found to have stronger magnitudes of FDs while stations with higher rigidity were found to have a weaker magnitude of FDs. Therefore, our findings agree with the suggestion that FD magnitudes vary inversely with the station's rigidity.

Similarly, strong and positive correlations were found to exist among the FDs of the CR stations under study. Additionally, a strong and significant correlation was found between FD magnitudes with interplanetary magnetic field.

The contribution to knowledge from this study is that it generated a large catalogue of FDs which will be used to carry out further studies on Forbush decrease.

5.2Conclusion

The influence of geomagnetic cutoff rigidity on Forbush decreases has been the subject of extensive investigation. An analysis of daily cosmic ray (CR) counts from the TIBT and MGDN stations revealed a significant decrease in cosmic ray intensity, known as a Forbush decrease events. This study identified a noteworthy relationship between the magnitudes of Forbush decreases and the corresponding cutoff rigidity. It suggests that Forbush decreases are influenced by the rigidity levels of cosmic ray stations, indicating that the magnitudes of these decreases tend to vary inversely with the station's rigidity. This finding contributes valuable insights into the dynamics of cosmic rays and their interaction with the Earth's magnetic field.

REFERENCES

[1] Ahluwalia, H.S., Ygbuhay, R.C., and Duldig, M.L. (2009). Two intense Forbush decreases of solar activity cycle 22. *Adv. Space Res.*, 44, 58. DOI.
[2] Aguilar, M., Ali Cavasonza, L., Alpat, B., *et al.,* (2016). Antiproton Flux, Antiproton-to- Proton Flux Ratio, and Properties of Elementary Particle Fluxes in Primary Cosmic Rays Measured with the Alpha Magnetic Spectrometer on the International Space Station. *Physical Review Letters*, 117, 091103.
[3] Aguilar, M., Ali Cavasonza, L., Ambrosi, G., *et al.,* (2018). Observation of Fine Time Structures in the Cosmic Proton and Helium Fluxes with the Alpha Magnetic Spectrometer on the InternationalSpace Station. *Phys. Rev. Lett.,* 120 021101.
[4] Ahlers and Mertsch (2015). Small-Scale Anisotropies of Cosmic Rays from Relative Diffusion. *Phys. Rev. Lett*, arXiv:1506.05488 [astro-ph.HE].
[5] Ahluwalia H. S. and Fikani M. M. (2007). Cosmic ray detector response to transient solar Modulation: Forbush decreases. *Journal of geophysical research,* 112, (A8)
[6] Albert, J., *et al.,* (2007). Very high energy gamma-ray radiation from the stellar mass black hole binary Cygnus X-1. *Astrophys. J. Lett.* 665, L51–L54. https://doi.org10.1086/521145.
[7] Aartsen M. G., Abbasi R., AbdouY., and M. Ackermann (2014). Observation of the cosmic-ray shadow of the Moon with IceCube. *Physical Review D*, 89(10), 102004
[8] Badruddin N. (2002). Transient modulation of cosmic ray intensity: Role of magnetic clouds and turbulent interaction regions. *Astrophys. Space Sci.,* 281, 651–661.
[9] Balco, G., (2011). Contributions and unrealized potential contributions of cosmogenic- nuclide exposure dating to glacier chronology, 1990-2010. *Quaternary Science Reviews*, 30(1-2), 3-27.
[10] Benyamin, D., Nakar, E., Piran, T., and Shaviv, N. J. (2016). The B/C and Sub-iron/Iron Cosmic Ray Ratios–Further Evidence in Favor of the Spiral-Arm Diffusion Model. *ApJ*, 826, 47.
[11] Belov, A., (2009). Universal heliophysical processes. In: Proceedings of the International Astronomical Union. *IAU Symposium 257*, 439–450.
[12] Belov A. V., Eroshenko E. A., Yanke V. G., Oleneva V. A., and Abunina M. A., (2018).

a. Global Survey Method for the World Network of Neutron Monitors. *Geomagnetism and Aeronomy*, 58, 356.

[13] Belov A., Athanasios P., Maria A., Dumbovic M., Richardson I. G., Heber B., Kuhl P., Herbst K., Anastasios A., Vourlidas A., Eroshenko E., and Artem A. (2021). On the Rigidity Spectrum of Cosmic-Ray Variations within Propagating Interplanetary Disturbances: Neutron Monitor and SOHO/EPHIN Observations at ∼1–10 GV. *The Astrophysical Journal*, 908(5), 14

[14] Belov, A.V., Eroshenko, E.A., Oleneva, V.A., Struminsky, A.B., Yanke, V.G., (2001b).

[15] What determines the magnitude of Forbush decreases? *Advances in Space Research,* 27, 625–630.

[16] Belov, A.V., Eroshenko, E.A., Oleneva, V.A., Yanke, V.G., (2008). Connection of Forbush effects to the X-ray flares. *Journal of Atmospheric and Solar-Terrestrial Physics,* 70, 342–350

[17] Belov, A., Abunin, A., Abunina, M., Eroshenko, E., Oleneva, V., Yanke, V., Papaioannuou, A., Maromichalaki, H., Gopalswamy, N., Yashiro, S., (2014). Coronal mass ejections and non-recurrent Forbush decreases. *Sol. Phys.,* 289 (10).

[18] Belov, A.V., Eroshenko, E.A., Yanke, V.G., Oleneva, V.A., Abunina, M.A., A., A.A., (2018). Global survey method for the world network of neutron monitors. *Geomagn. Aeron*, 58 (3), 356–372.

[19] Benjamin Laken, Dominic Kniveton, and Arnold Wolfendale (2011). Forbush decreases, solar irradiance variations, and anomalous cloud changes. *Journal of Geophysical Research*, 116, D09201.

[20] Bhaskar, B., Subramanian, P., and Vichare, G. (2016). Relative contribution of the magnetic field barrier and solar wind speed in ICME-associated Forbush decreases. *Astrophys. J.* 828, 104. DOI.

[21] Bieber, J.W., Eroshenko, E., Evenson, P. *et al.* (2000). Cosmic Rays and Earth – A Summary. *Space Science Reviews* 93, 1–9. https://doi.org/10.1023/A:1026515722112.

[22] Buchvarova, M. and Velinov, P. (2005). Modeling spectra of cosmic ray influencing on the ionospheres of the earth and outer planets during solar maxium and minimum. *Advances in Space Research,* 36, 2127 – 2133. 10.1016/j.asr.2005.04.002.

[23] Bütikofer, R. (2018). Cosmic Ray Particle Transport in the Earth's Magnetosphere. In: Malandraki, O., Crosby, N. (eds) Solar Particle Radiation Storms Forecasting and Analysis. Astrophysics and Space Science Library, vol 444. Springer, Cham. https://doi.org/10.1007/978-3-319-60051-2_5

[24] Cane H.V. (2000). Coronal mass ejections and Forbush decreases. *SSRv* 93, 55–77. http://dx.doi.org/10.1023/m7.

[25] Cane, H.V., Richardson, I.G., von Rosenvinge, T.T., (1996). Cosmic ray decreases: 1964–1994. *Journal of Geophysical Research,* 101, 21561–21572.

[26] Cane, H. V., Richardson, I. G., von Rosenvinge, T. T., and Wibberenz, G. (1994). Cosmic ray decreases and shock structure: A multispacecraft study. *JGR,* 99(11), 21429-21441

[27] Cane, H.V., Richardson, I.G. and von Rosenvinge, T.T. (1996). Cosmic ray decreases: 1964 – 1994. *J. Geophys. Res.* 101(A10), 21561.

[28] Carmichael, H., Shea, M. and Peterson, R.. (2011). III. Cosmic-ray latitude survey in Western USA and Hawaii in summer, 1966. *Canadian Journal of Physics,* 47. 2057-2065. 10.1139/p69-259.

[29] Carroll, B. W., and Ostlie, D. A. (2017). An Introduction to Modern Astrophysics (2nd ed.). Cambridge: Cambridge University Press.

[30] Chaisson, Eric and McMillan, Stephen. (2014). Astronomy Today. McMillian Press, USA.

[31] Chree, C. (1912). Some phenomena of sunspots and of terrestrial magnetism, at Kew Observatory. *Philos. Trans. Roy. Soc. London, Ser. A, Contain. Pap. Math. Phys. Character,* 212, 484.

[32] Cockburn, H.A.P. and M.A. Summerfield (2004). Geomorphological applications of cosmogenicisotope analysis. *Progress in Physical Geography,* 28(1), 1-42.

[33] Demorest, P. (2001). Dynamo theory and Earth's magnetic field. Retrieved from https://pdfs.semanticscholar.org/351e/344c1a92e7f20ae3d419f37cef59117eecb8. pdf.

[34] Du Z. L. (2011). The Correlation between Solar and Geomagnetic Activity – Part 1; Two term decomposition of geomagnetic activity. *Journal Annales Geophysical,* 29(35), 1331-1340.

[35] Finlay, C. C., Maus, S., Beggan, C. D., Bondar, T. N., Chambodut, A., Chernova, T. A., and Zvereva, T. I. (2010). International Geomagnetic Reference Field: the eleventh generation. *Geophysical Journal International,* 183, 1216–1230.

[36] Genolini Y., Pasquale D. S., Mathieu B. *et. al.,* (2017). Indications for a high- rigidity break in the cosmic-ray diffusion coefficient. *Physical Review Letters,* 11910.1103/PhysRevLett.119.241101.

[37] Harrison R. Giles, Maarten H.P. Ambaum, (2010). Observing Forbush decreases in cloud at

[38] Shetland. *Journal of Atmospheric and Solar-Terrestrial Physics,* 72(18)1408-1414.

[39] Ihongo, G.D., Wang, and C.H.T (2016). The effects of solar wind on galactic cosmic ray flux at Earth. *Astrophys Space Sci,* 361**,** 44.https://doi.org/10.1007/s10509-015- 2628-5.

[40] Jamsen, T., Usoskin, I.G., Raiha, T., Sarkamo, J., and Kovaltsov, G., (2007). Case study of Forbush decreases energy depandance of the recovery. *Advances in Space Research,* 40, 342–347.

[41] Kalugin G. and Kabin K. (2015). An analysis of large Forbush decrease events using phase diagrams of view channels of the Nagoya multidirectional muon telescope. *Journal of Atmospheric and Solar-Terrestrial Physics,* 123, 124-136.

[42] Kane, R.P., (2010). Severe geomagnetic storms and Forbush decreases: interplanetary relationships re-examined. *Ann. Geophys*., 28, 479–489.

[43] Kristjansson, J. E., Stjern, C.W., Stordal, F., Fjaraa, A.M., Myrhre, G., and Jonasson, K. (2008). Cosmic rays, cloud condensation nuclei and clouds – a reassessment using MODIS data. Atmos. *Chem. Phys. Discuss.* 8, 13265. DOI.

[44] Kumar and Eichler (2014). Large-Scale Anisotropy of TeV-Band Cosmic Rays. *The Astrophysical Journal*, 785,129.

[45] Lee S.S., Oh S.Y. and Yi Y. (2013). Simultaneity of Forbush decrease events observed at middle-latitude neutron monitor. *JGR* 118, 608-614

[46] Lee S., Oh S., Yi Y., Evenson P., Jee G., and Choi H. (2015). Long-term Statistical Analysis of the Simultaneity of Forbush Decrease Events at Middle Latitudes. *J. Astron. Space Sci.,* 32(1), 33-38

[47] Lingri, D., Mavromichalaki, H., Belov, A., Eroshenko, E., Yanke, V., Abunin, A., and Abunina, M. (2016). Solar activity parameters and associated Forbush decreases during the minimum between Cycles 23 and 24 and the ascending phase of Cycle 24. *Solar Phys.*, 291(3), 1025.

[48] Lockwood J. A., Webber W.R. and Debrunner H. (1991a). Forbush decreases interplanetary magnetic field disturbances: Association with magnetic clouds, *JGR*, 96, 11587–11604. http://dx.doi.org/10.1029/91JA01012.

[49] Lockwood, J.A. and W.R. Webber (1967). Differential response and specific yield functions of cosmic-ray neutron monitors. *J. Geophys. Res.,* 72, 3395.

[50] Lockwood, J. A., J. Lezniak, P. Singh, and W.R. Webber (1970). Rigidity dependence for Forbush decreases in 1968 compared with that for the 11-year variation, *J. Geophys. Res.,* 75, 6885.

[51] Lockwood, J.A., W. R. Webber, and J. R. Jokipii (1986). Characteristic recovery times of Forbush-type decreases in the cosmic radiation, 1, Observations at Earth at different rigidities. *J. Geophys. Res.*, 91,2851.

[52] Lockwood, J.A., H. De-brenner, E.O. Fliickiger, and H. Gradel (1990). Proton energy spectra at the Sun during the May 7, 1978, and February 16, 1984, solar cosmic ray events, *Astrophys. J.,* 355, 287.

[53] Lockwood, J. A., Webber, W. R. and Debrunner, H., (1991b). the rigidity dependence of forbush decreases observed at the earth. *J. Geophys. Res.,* 96, 5447.

[54] Mason, P. A., McNamara, B. J. and Harrison, T. E., (1997). High energy transient events from Cygnus X-1: evidence for a source of galactic gamma-ray bursts. *Astron. J.* 114, 238. https://doi.org/10.1086/118468.

[55] Mirabel, I. F., Dijkstra, M., Laurent, P., Loeb, A. and Pritchard, J. R., (2011). Stellar black holes at the dawn of the universe. *Astron. Astrophys.* 528, A149. https://doi.org/ 10.1051/0004- 6361/201016357.

[56] Ngobien M. D. (2006). The aspect of the modulation of cosmic rays in the outer heliosphere, Northwest University, South Africa, 182-204 Oh S.Y., Yi Y. and Kim Y.H. (2008). Globally nonsimultaneous Forbush decrease events and their implications. *JGR* 113, A01103. http://dx.doi.org/10.1029/2007JA012333
[57] Oh S.Y., Yi Y., (2009). Statistical Reality of Globally Nonsimultaneous Forbush Decrease Events, *JGR* 114, A11102. http://dx.doi.org/10.1029/2009JA014190.
[58] Oh, S. Y., J. W. Bieber, J. Clem, P. Evenson, R. Pyle, Y. Yi, and Y.-K. Kim (2012). South Pole neutron monitor forecasting of solar proton radiation intensity. *Space Weather,* 10, S05004. doi:10.1029/2012SW000795.

[59] Okike, O. and Collier, A.B. (2011a). A multivariate study of Forbush decrease simultaneity.*J. Atmos. Solar-Terr. Phys.* 73, 796.
[60] Okike O. and Nwuzor O. C. (2020). Investigation of the rigidity and sensitivity dependence of neutron monitors for cosmic ray modulation using algorithm-selected Forbush decreases. *MNRAS* 493, 1948–1959.
[61] Okike O. (2020). Automated detection of simultaneous/non-simultaneous Forbush decreases and the associated cosmic ray phenomena, *Journal of Atmospheric and Solar-Terrestrial Physics*, 211,1364-6826
[62] Okwonu F. Z., Asaju B. L. and Arunaye F. I. (2020). Breakdown Analysis of Pearson Correlation Coefficient and Robust Correlation Methods. *IOP Conf. Ser.: Mater. Sci. Eng*., 917 01206.
[63] Pohl H. and Eichler G. (2013). Understanding TeV-band cosmic-ray anisotropy. *The Astrophysical Journal*, 766:4, 9.
[64] Pyle K. R., (1997). Neutron monitor sensitivity to solar modulation changes: altitude vs. cutoff rigidity. *In Proc. 25th Int. Cosmic Ray Conference, World Scientific, Singapore,* 343
[65] Richardson, I. G. (2004). The fraction of interplanetary coronal mass ejections that are magnetic clouds: Evidence for a solar cycle variation. *Geophysical Research Letters*, 31 (18). doi:10.1029/2004gl020958
[66] Richardson, J., Atherton Day, N., Peacock, S., and Iezzi, A. (2004). Measurement of the Quality of Life for Economic Evaluation and the Assessment of Quality of Life (AQoL) Mark 2 Instrument. *The Australian Economic Review,* 37(1), *62–88.* doi:10.1111/j.1467-8462.2004.00308.x.
[67] Shea, M. A., and Smart, D. F. (1983). A world grid of calculated cosmic ray vertical cutoff rigidities for 1980. *Proceedings of the 18th International Cosmic Ray Conference*, 3, 415–418.
[68] Shea, M. A., Smart, D. F., and McCall, J.R. (1968). A five-degree by fifteen-degree world grid of trajectory determined vertical cutoff rigidities. *Canadian Journal of Physics,* 46, S1098–S1101.
[69] Shea M.A. and Smart D.F. (2006). Geomagnetic cutoff rigidities and geomagnetic coordinates appropriate for the Carrington flare Epoch. *Advances in Space Research,* 38 209–214.
[70] Singh, M., and Badrddin, N. (2006). Study of the cosmic ray diurnal anisotropy during different solar and magnetic conditions. *Sol. Phys.*, 233, 291–317.
[71] Smart, D. F., and Shea, M. A. (1997). World grid of calculated cosmic ray vertical cutoff rigidities for epoch 1990. *Proceedings of the 25th International Cosmic Ray Conference,* 2, 401–404.
[72] Smart, D. F., and Shea, M. A. (2001). Geomagnetic cutoff rigidity computer program. Final report. Grant NAG5-8009. https://ccmc.gsfc.nasa.gov/modelweb/sun/cutoff.html.
[73] Smart, D. F. (2005). Vertical Geomagnetic Cutoff Rigidity Latitude Plots: IGRF 2000 (Report No. AC-04-02566). Federal Aviation Administration, Civil Aerospace Medical Institute.
[74] Smart, D. F., and Shea, M. A. (2008). World grid of calculated cosmic ray vertical cutoff rigidities for epoch 1995.0. *Proceedings of the 30th International Cosmic Ray Conference,* 1, 733–736.
[75] Smart, D. F., and Shea, M. A. (2013). Final Report: Vertical Geomagnetic Cutoff Rigidities for Epoch 2010 (Report No. DTFAAC-12-P-06334; FAA Procurement AAM-610-12-0157). Federal Aviation Administration.
[76] Simpson, J. A. (2000). The cosmic ray nucleonic component: The invention and scientific uses of the neutron monitor. *Space Science Reviews*. 93 (1/2): 11–32.
[77] Tanabashi M. *et al.* (2018). Cosmic rays, *Phys. Rev.* D 98, 030001
[78] Tezari, A., Mavromichalaki, H. (2016). Diurnal anisotropy of cosmic rays during intensive solar activity for the period 2001 – 2014. *New Astron.,* 46, 78. DOI.
[79] Todd, M.C and Kniveton, D.R. (2001). Changes in cloud cover associated with Forbush decreases galactic cosmic rays. *Journal of Geophysical Research-Atmospheres*,
[80] 106 (D23) 32031 – 32042. 10.1029/2001JD000405.
[81] Webber W. (1962). The production of free electrons in the ionospheric D layer by solar and galactic cosmic rays and the resultant absorption of radio waves. *Journal of Geophysical Research*, 67(13),5091-5106.
[82] Webber, W., Lockwood, J. (1998). The Inner Heliosphere- Outer Heliosphere Comparison for Cosmic Ray Modulation. *Space Science Reviews*, 83, 159–167. https://doi.org/ 10.1023/A:1005018823031
[83] Webber W. R. and J. A. Lockwood (1991). An observation of a heliospheric magnetic cycle dependence for the integral radial gradient of E > 60 MeV cosmic rays. *Journal of Geophysical Research*, 97(46),8221-8230.